Bladed Disk Crack Detection through Advanced Analysis of Blade Passage Signals

by

Elhamo Sadat Alavi Foumani, B.Sc.

Directed by

Dr. Ming Liang

Dr. Jie Liu

A thesis submitted to the Faculty of Graduate and Postdoctoral studies
In partial fulfillment of the requirements for the degree of
MASTER OF APPLIED SCIENCE
in Mechanical Engineering

Ottawa- Carleton Institute for Mechanical and Aerospace Engineering

University of Ottawa

ABSTRACT

Crack initiation and propagation in the bladed disks of aero-engines caused by high-cycle fatigue under cyclic loads could result in the breakdown of the engines if not detected at an early stage. Although a number of fault detection methods have been reported in the literature, it still remains very challenging to develop a reliable online technique to accurately diagnose defects in bladed disks. One of the main challenges is to characterize signals contaminated by noises. These noises caused by very dynamic engine operation environment. This work presents a new technique for engine bladed disk crack detection, which utilizes advanced analysis of clearance and time-of-arrival signals acquired from blade tip sensors. This technique involves two stages of signal processing: 1) signal pre-processing for noise elimination from predetermined causes; and 2) signal post-processing for characterizing crack initiation and location. Experimental results from the spin rig test were used to validate technique predictions.

ACKNOWLEDGEMENTS

I would like to acknowledge people who made this work possible. First and foremost, I would like to sincerely thank my supervisor and co-supervisor, Dr. Ming Liang and Dr. Jie Liu for their support, guidance, encouragement and knowledge.

I would also like to extend a heartfelt thanks to Hooman Hanachi for all his efforts in the research group to provide better research environment and all his kindness during the period that I was working on this project.

Furthermore, this project was supported by the Natural Sciences and Engineering Research Council (NSERC) of Canada, and the Life Prediction Technologies Inc (LPTi), Ottawa, Canada that I would like to thank them.

Moreover, I would like to express my deepest appreciation to my family for all their understanding and support throughout my studies specially my mother and my father.

Table of Contents

List of Figures

CHAPTER ONE

INTRODUCTION

1.1. OVERVIEW

The development of reliable health condition monitoring systems has long been the focus of various undertakings in a wide array of industries to prevent machine performance degradation, malfunction, or even catastrophic failures [1-3]. The most recent Deep-water Horizon Oil Spill in the Gulf of Mexico demonstrated that an unexpected equipment failure can potentially result in not only the loss of productivity but also the loss of expensive equipment and possibly human lives and environmental resources [3, 4].

Aero-engines are widely used for aircraft propulsion. High speed rotating engine components store a huge amount of kinetic energy in operation and are susceptible to many kinds of problems [3]. Some of principal bladed disks faults are given as below:

- Looseness [5]
- Distortion [6]
- Fatigue [2, 7, 8, 11]
- Erosion [10]
- Crack [2, 11-13]
- Manufacturing problems [13]

One of the problems that have plagued the engine manufacturers for decades is the failures due to high cycle fatigue in bladed disks [8, 11]. High cycle fatigue failures typically have a root cause which stems from flaws in the material (impurities or voids), abusive machining which creates high stress concentrations, or wear between components [14]. However, even "perfect" components have a finite life, and will fail after a certain number of cycles [3, 13]. If a fatigue crack develops in the blades or disks, it will significantly affect the whole engine function as well as the safety of the relevant aircraft system [3, 8]. In practice, typical failures in aero-engines are related to crack initiation and propagation around dovetail regions of bladed disks [15].

The cracks usually propagate under cyclic load and end up to abrupt part breakage which may create more damages to other components leading to system shutdown. In addition to maintenance costs, the aircraft remains non-operative during repair time, which leads to more economical loss [2]. In order to prevent such costly damages, time-based inspection and maintenance of the system is often adopted. Despite some advantages, this method can be uneconomical as a number of unnecessary but costly inspections are carried out and some engine components may be prematurely replaced, which otherwise could be safely operated for a longer time. In order to extend the useful life of the components while assuring the overall system performance is safe and acceptable, condition-based maintenance is usually an effective alternative where a reliable in-situ health monitoring of the system is the key [1- 3, 8, 16].

1.2. LITERATURE REVIEW

This section reviews the state of the art related to bladed disk fault detection and feature extraction using signal processing methods.

1.2.1. BLADED DISK CRACK MEASUREMENT METHODS

There are several approaches proposed in the literature for crack detection in bladed disks of aero-engines while the engine is in operation.

- Vibration Measurement

Any rotary component failure causes an abnormal vibration in a rotary machine. As a result, vibration measurement has become a powerful tool in machinery condition monitoring. Many techniques are proposed for this purpose [2, 8, 11, 13, 17]. One method suggests extracting blade vibration signature from the main shaft vibration signal by using a torsional vibration transducer and detecting potential cracks [11, 21]. Among recent methods for blade vibration measurment and analysis is the "blade tip timing" measurement [8]. In this method the travel time of the blade between case mounted electromagnetic or stationary optical probes is measured, due to the fact that the passing time varies with the blade vibration [12, 22]. An advanced application of this method was the development of an optical semiconductor blade vibration monitoring system to estimate the health condition of the fan blades, compressor blades, and turbine blades by measuring the vibration level of corresponding parts [23]. This method was validated through different

platforms [2, 8, 11]. Another approach is based on the fact that vibration of a rotating blade excites a pressure wave which could be measured by a microphone [22].

- Acoustic Measurement

One of the most effective acoustic based bladed disk condition monitoring is the "acoustic emission". Deformation or damage within or on the surface of a material causes a release of strain energy which generates transient elastic waves named acoustic emission (AE). In rotary machines, transient elastic waves emitted by the interaction of two media in relative motion [3, 24, 25].

- Blade Position Measurement

Another approach suggests measuring position of the blades as an indicative parameter for detecting cracks in the blade dovetail roots. In practice, for measuring length and axial position of the blades, measurements are carried out on blade "tip clearance" and "time of arrival" consequently [2, 26]. In some researches, blade tip sensors were used for measuring blade tip clearance as well as blade vibration [2, 27, 28]. The performance of Capacitance sensors relies on clearance of the blade tip's access and the consistency of fluid's dielectric in the gap between sensor and blade. Moreover, these sensors are very sensible to temperature variations, and surface contamination by oil [28, 29]. Similarly, for optical devices clearance of access to the blade tip and transparency of the fluid in the gap are required. Unlike the capacitance sensors, the optical devices can perform at very high temperatures

although the presence of contaminants can still impair their data. In comparison to aforementioned devices, eddy current sensors are less sensible to clearance of access to blade or the presence of oil and other contaminants. These sensors can carry out the measurements for both tip timing and tip clearance of blades in real time at very high resolution. However, the thickness and the type of material can reduce the performance [29, 30]. Also, there were autonomous algorithms developed for the real-time analysis of time of arrival [2, 31] and tip clearance data [9].

In this work, tip clearance and time of arrival signals of an aero-engine bladed fan disc, generated by capacitance tip sensors are measured. Consequently, further signal processing techniques are employed for extracting features and diagnosis of any possible fault in the blades and/or disk.

1.2.2. SIGNAL PROCESSING TECHNIQUES FOR BLADED DISK CRACK DETECTION

Since any defect in a bladed disk, either the defects related to individual blades or the rotor disk can affect the blade passage signal, signal processing methods can be employed in the bladed disk health monitoring [27].

According to the rotary motion of an aero-engine bladed fan disc, the blade positioning signals are periodic. As a result, vibration-based signal processing can be performed for these kinds of signal. Vibration base signal processing methods are categorized according to the domain they are applied in; the time domain [1, 4, 33], the frequency domain [1, 7, 34, 35] and the time-frequency domain [1, 34, 36- 40].

In many cases, the techniques are complementary and are not totally independent [1, 36, 17].

In the time domain analysis, one is interested in the variation of some statistical indices in the data set in signal such as root mean square (RMS), kurtosis, skewness, or the standard deviation. The advantages of time domain analysis are simple calculations, straightforward signal pre-processing, and speed independency. However, it has some drawbacks such as insensitivity to early stage faults and deeply distributed defects [33, 41- 43].

The most reported signal processing method is frequency domain, also called spectral analysis. In this approach, the fault detection is based on the spectral information analysis. The machine health condition is monitored in the spectra or in some extended spectral terminology such as the bispectrum map [35, 44, 45] and power spectrum [53]. This method has the advantage over the time domain analysis that it is easier to detect and setting apart certain frequency components of interest while it is not appropriate to analyze the non-stationary or transient signals which are the case in many machine defects [25, 34].

The time-frequency domain analysis is the suggested method to study non-stationary signals. There are several techniques proposed in literature for applying time-frequency domain analysis such as the short-time Fourier transform (STFT) [1, 37, 39, 40], the Wigner-Ville distribution [40], and the wavelet transform (WT) [17-20, 44, 47, 56]. Due to its flexibility and computational benefits and its ability in signal feature extraction, the wavelet transform has attracted growing interests in

recent years. The approach can be categorized as the continuous wavelet [17, 44, 48, 49, 50], the discrete wavelet [29, 44], the wavelet packet analysis [30, 41], and those WTs with post-processing analysis such as the FT [36, 38, 47, 50, 54] and the energy density analysis [38].

1.3. OBJECTIVES

Although a number of methods have been reported in the literature, engine bladed disk crack detection is still a challenging task in both research and real-world applications [22, 55]. This is mainly because: a) turbine engines operate in a very dynamic environment and the changes in this environment affect the behavior of the turbine system; and b) the engine components are inaccessible for direct measurement, and nondestructive testing methods are usually applied to estimate the health condition of the bladed disks. Accordingly, the aim of this work is to develop a novel signal processing technique to take on this challenge and provide a more reliable technique and tool for rotating bladed disc crack detection that can be applied in a wide array of industries. The purpose is to detect and locate the bladed disk faults by using Wavelet transform method and also deterended flactuation analysis.

1.4. THESIS OUTLINE

This work presents a novel technique for bladed disc crack detection through two sequential signal processing stages: 1) Signal preprocessing that aims to eliminate the noises carried by the blade passage signals and induced respectively by thermal

and centrifugal expansions, rotor imbalance, and shaft bending effects; and 2) signal postprocessing that intends to extract the crack features and identify its location. In the first stage, physics-based modeling and interpretation are established to help characterize the noises. The crack initiation can be determined based on the calculated health monitoring index derived from the sinusoidal effects. In the second stage, the crack is located through statistical wavelet analysis and the advanced detrended fluctuation analysis of the preprocessed data.

The proposed technique is validated using a set of spin rig test data (i.e., tip-clearance and time-of-arrival) that was acquired during a test conducted on an aero engine bladed fan disc. The suggested technique is new in the following aspects: 1) the physics-based modeling and interpretation are established to characterize the noises induced by thermal and centrifugal expansions, rotor imbalance, and shaft bending effects; these noises have been eliminated from the original signal in the signal preprocessing stage to augment the signal-to-noise ratio (SNR); 2) the crack initiation time can be determined using the suggested health monitoring index derived from the sinusoidal effects; 3) the detrended fluctuation analysis (DFA) is proposed for crack location identification.

This thesis is organized as follows. The suggested signal preprocessing technique for signal denoising and crack initiation determination is presented in Chapter Two. The suggested statistical wavelet analysis for engine crack detection is described in Chapter Three and the proposed DFA based technique for crack location

identification is proposed in Chapter Three as well. Some concluding remarks are summarized in Chapter Four.

CHAPTER TWO

SIGNAL PREPROCESSING FOR NOISE REMOVAL

2.1 INTRODUCTION

Health condition monitoring and fault diagnostics of aero-engines play significant roles in cost reduction and reliability enhancement of the aircraft systems. Among various types of potential faults in an aero-engine, crack initiation and propagation in engine bladed discs caused by high-cycle fatigue under cyclic loads are typical ones that could result in the breakdown of the engines if not detected at an early stage. Reliable fault detection techniques are therefore in demand to prevent engine malfunctions as well as unexpected failures that could lead to costly and/or catastrophic consequences [1, 2].

Bladed disc fault diagnostics involves two sequential processes: feature extraction and fault detection. Feature extraction is a process in which the bladed disc health condition related features are extracted by appropriate signal processing techniques, whereas fault detection is a decision-making process to estimate bladed disc health conditions based on the extracted representative features. Feature extraction therefore plays a significant role for bladed disc fault diagnostics whereas non-robust features may lead to false alarms (i.e., an alarm is triggered by some noise instead of a real bladed disc fault) or missed alarms (i.e., the diagnostic tool cannot recognize the existence of a bladed disc defect) [47, 54, 56].

In this work, a set of spin rig test data was acquired during a test conducted on an aero engine bladed fan disc. A wire-EDM notch was pre-built into the dovetail region of the bladed disc beneath the 32nd and 33rd blades. The crack started its propagation when the testing reaches the 500th data recording cycle. The physical interpretation for measuring these two types of signals for bladed disc crack detection is given next. The proposed advanced signal analysis will be conducted on these blade passage data to identify when and where the crack initiates its propagation. The effort was thus expanded in analyzing this fan data using some novel analytical procedures developed in the next chapter.

2.2. EXPERIMENTAL SETUP

Blade position measurement is suggested by some researchers in the literature to detect the indicative parameter of crack in the blades [6, 7, 8, 9]. Blade tip sensors are employed to carry out the measurement on blade position in the spin rig test. The fan disc was mounted on the spin rig and driven by a motor in a vacuum chamber (1.2 m diameter × 1.2 m deep, approximately 100 millitorr in operation) with the rotational speed ranging between 3000 to 3600 rpm with a variation of around 1%. The spin rig is equipped with a programmable logic control (PLC) system that ensures safe and fool-proof operation. The data measured during the spin rig test about the tip clearance and time of arrival of 40 blades during 1408 data recording cycles have been collected using a capacitance probe technique with the sampling frequency 50 kHz

- **SPIN RIG TEST FACILITY**

The spin rig facility is used to test gas turbines components, as well as other rotating components and assemblies (Fig. 2.2). This facility examines performance, strength, durability and damage tolerance under cyclic, steady-state or combined centrifugal loads, at ambient as well as elevated temperatures. The adaptable system can simulate the effect of fatigue and creep loads in a programmable sequence through a wide range of test types. It uses high accuracy air drive and breaking turbines to control loading and unloading rates. As a result, light-weight to very heavy components and component assemblies can be tested at high rotational speeds and high temperatures.

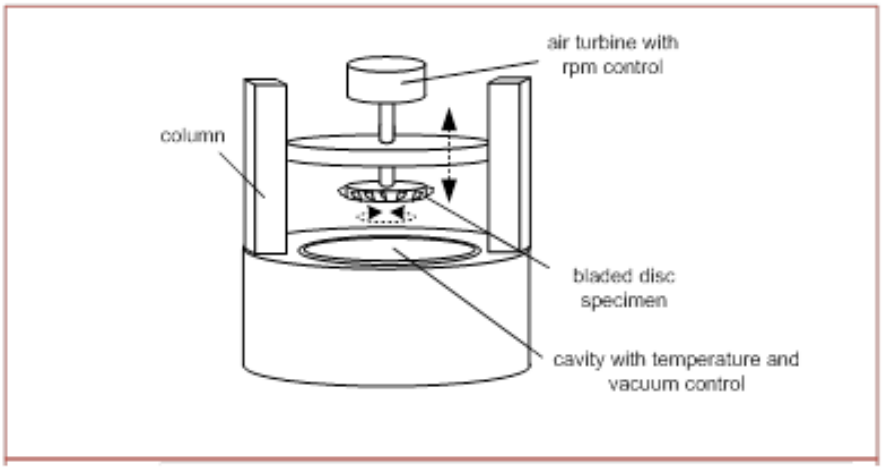

Fig. 2.2 Lowering a turbine disk into the spin rig

Spin rig test facility has the capability of:

- performance tests under cyclic and/or steady-state loads to demonstrate a design or qualify a rotating part or rotating assembly

- cyclic or steady-state tests to experimentally determine the fracture-critical locations in rotating components
- cyclic or steady-state durability tests to experimentally determine fatigue or creep crack initiation life
- damage tolerance tests to demonstrate crack propagation resistance of rotating parts and to verify safe inspection intervals
- Increasing centrifugal load tests to determine the burst strength and over-speed margin of rotating components.

In this work, the data about the tip clearance and time of arrival of 40 blades during 1408 data recording cycles have been collected using capacitance probes with the sampling frequency 50 kHz, as schematically shown in Fig. 2.3.2 (a).

2.3. Signal Denoising and Crack Initiation Determination

2.3.1. Tip Clearance Signal Analysis

The *Tip Clearance* (TC) data indicate the distance between the tip of the sensing unit and the tip of the engine blades and is used in this study for analysis in bladed disc crack detection. As illustrated in Fig. 2.3.2 (b), the blades in a healthy engine are stretched out when spinning up and retracted when spinning down due to centrifugal effect. The variation in the length of the blades is limited in a relatively constant band after a few cycles of spinning-up and spinning-down operation. However, when an incipient crack occurs in a rotating disc, the effective cross-section of the material reduces, and therefore the stiffness decreases as well. The

elastic deformation is intensified in comparison with normal condition and consequently a plastic deformation happens in the cracked region due to stress concentration. The plastic deformation does not completely retract when the engine is decelerated and thus an increasing trend of elongation in engine operation. The blade length keeps increasing with cycles when there is a crack occurring in the bladed disc and accordingly an abnormal increase in the length of a blade can be interpreted as a reasonable signature for crack initiation and propagation.

2.3.2. TIME OF ARRIVAL SIGNAL ANALYSIS

The *Time of Arrival* (ToA) data indicate the time instants when the tip of a blade has a shortest distance with the tip of the sensing unit. Whenever a crack occurs within or underneath a blade, the rigidity of that blade declines due to the reduction in effective cross section. Such a blade is subject to more axial deflection under the aerodynamic loading caused by the hot gas flow. As a consequence, the damaged blade exhibits an axial displacement of Δx relative to a healthy one, as indicated in Fig. 2.3.2(c). The axial deflection of the blade leads to a virtually circumferential deflection dy due to the mounting angle α of the blade:

$$\Delta y = \Delta x / \tan \alpha \tag{2.3.2.1}$$

This leads to a shorter time of arrival Δt for the damaged blade:

$$\Delta t = \Delta y / (R\ \omega) = \Delta x / (R\ \omega \tan \alpha) \tag{2.3.2.2}$$

Suppose the designed time interval between the ToAs of two adjacent blades is t , the time interval before and after the damaged blade will become $t_1 = t - \Delta t$ and $t_2 = t + \Delta t$, respectively. This variation in the ToA could be a reasonable indicator for blade crack diagnostics. The trend of the parameter t could be correlated to the severity of crack propagation within a blade or a disc as well.

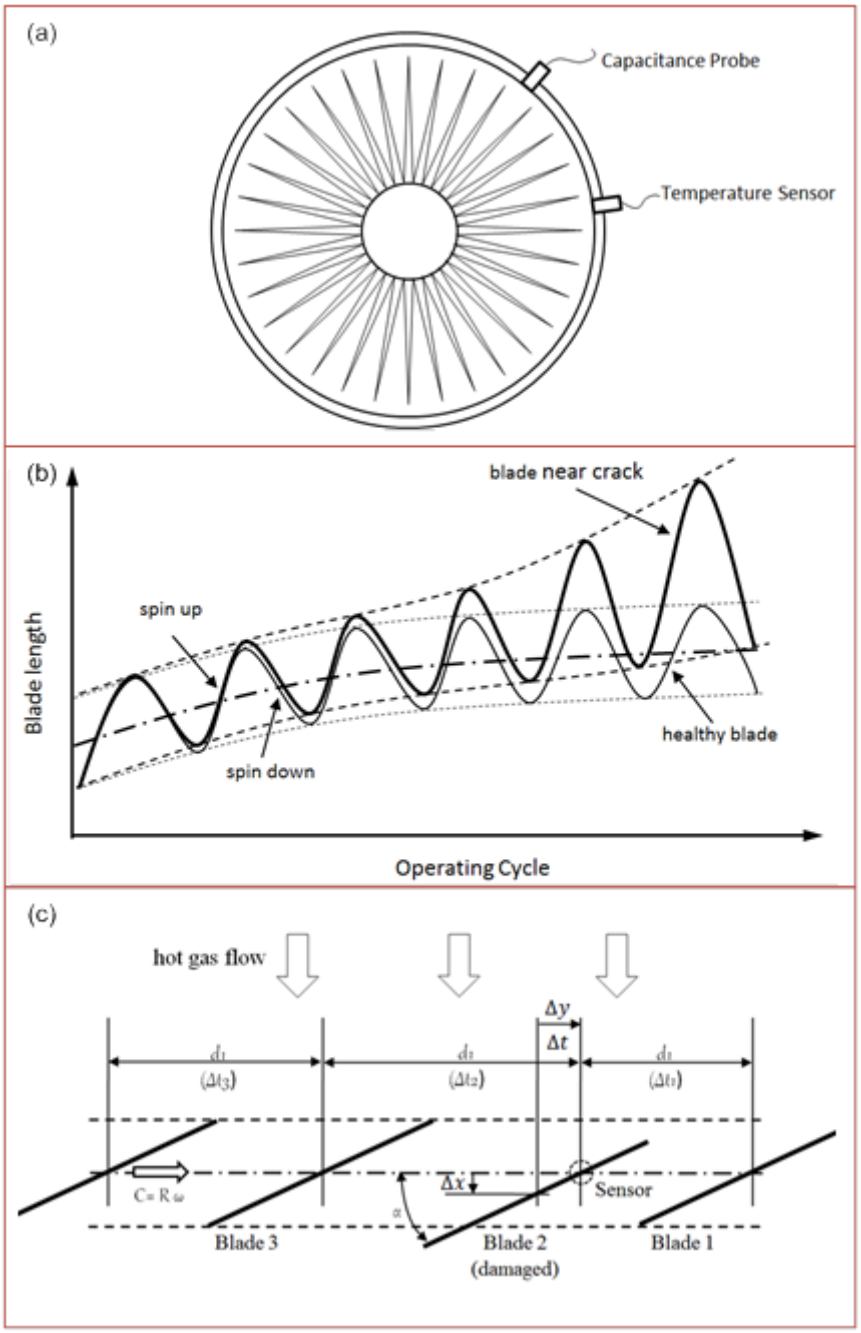

Fig. 2.3.2 (a) Measurement scheme for bladed disk crack detection; (b) the variation in blade length corresponding to different blade health conditions in operation; and (c) the axial deflection of a damaged blade can affect the ToA.

2.4. PREPROCESSING OF TC DATA

The signal analysis on the TC and ToA data represents the key step in effective feature extraction. The acquired blade passage signals usually contain both useful information and noise. Quite often, the useful information is severely contaminated by the background noise [21]. Signal preprocessing aims to reduce or eliminate the noises induced by some known factors so as to augment the SNR, thereby constituting an important step prior to further signal analysis.

In a spinning rotor, the blades are subject to thermal and speed-related centrifugal expansions that are not related to any defect. Considering the fact that the ambient temperature and the rotation speed remain relatively constant within a cycle, the variation in blade length caused by the aforementioned thermal and centrifugal effects is assumed to be identical for every blade. Accordingly, these effects can be eliminated from the signal by removing the average of the signal within the same cycle.

Another effect that needs to be considered is the influence caused by rotor imbalance. Although a turbine rotor is designed to be balanced and undergoes static and dynamic balancing process after assembling, there is always a minor residual imbalance that can become an important factor in high-speed rotations. This imbalance will cause a centrifugal force on the rotor shaft, acting as a bending moment, and such a bending effect will introduce a sinusoidal noise to the signal and should be eliminated prior to further signal analysis.

The periodic TC signal $f(i)$ (contaminated by noise) can be decomposed into the sum of a set of sinusoidal functions in which the first harmonic corresponds to the sinusoidal effect induced by the rotor imbalance:

$$f(i) = \frac{1}{2}a_0 + \sum_{n=1}^{\infty}\left(a_n \cos\frac{n\pi i}{m} + b_n \sin\frac{n\pi i}{m}\right) \tag{2.4.1}$$

where a_0 is the offset of the signal and a_n and b_n are coefficients of the nth harmonic. Correspondingly, the coefficients of the sinusoidal effect caused by the rotor imbalance are given by:

$$a_1 = \frac{2}{m}\sum_{i=1}^{m} f(i)\cos\left(\frac{2\pi\, i}{m}\right) \tag{2.4.2}$$

$$b_1 = \frac{2}{m}\sum_{i=1}^{m} f(i)\sin\left(\frac{2\pi\, i}{m}\right) \tag{2.4.3}$$

This sinusoidal effect is calculated within each data recording cycle and its magnitude and phase are given by $A_1 = ({a_1}^2 + {b_1}^2)^{1/2}$ and $\phi_1 = \tan^{-1}(a_1/b_1)$, respectively. Fig. 2.4 shows the computed amplitude and phase of the sinusoidal effect caused by the rotor imbalance in TC data. From Fig. 2.4, the following observations can be made:

1) The averages in both the amplitude and phase of this sinusoidal effect are nearly constant. This is reasonable because in the test the ambient temperature and the rotation speed (varying between 3613 RPM and 3641RPM) of the turbine

remain relatively constant during the spin rig test. Accordingly, the centrifugal force and the resulting bending moment exerted on the hub do not vary dramatically over time.

2) The localized standard deviation of both the amplitude and phase increase significantly around the 500^{th} data recording cycle. The abrupt changes in the magnitude and phase of the sinusoidal effect indicate the crack initiation. From a physical perspective, the crack initiation modifies the local stiffness of the disc that reshuffles the mass center of the rotor imbalance, and this subtle change can be well captured by observing the trend of the suggested localized standard deviation of the sinusoidal effect.

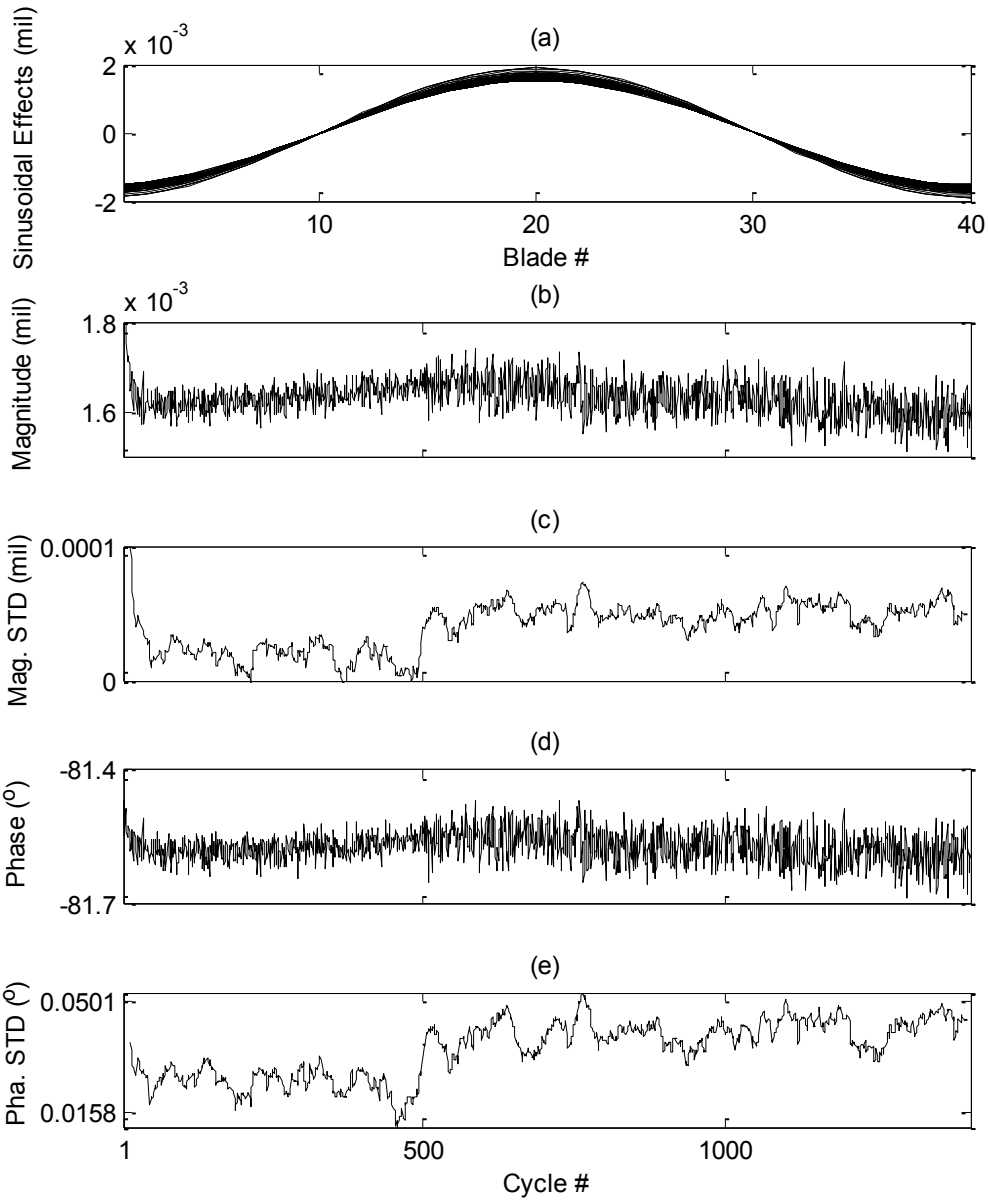

Fig. 2.4 The sinusoidal effects carried by the TC signal and caused by the rotor imbalance: (a) the sinusoidal effects over 1408 cycles; (b) the magnitude; (c) the localized standard deviation trend of the magnitudes; (d) the phase; and (e) the localized standard deviation trend of the phases.

2.5. PREPROCESSING OF TOA DATA

Any crack in the bladed disc can lead to variations in ToA that could carry useful information for crack detection. Prior to further analysis, a proper signal preprocessing procedure has to be taken to reduce or eliminate the interference caused by factors other than defects. As for the ToA data, the following considerations are made:

1) The average of ToA data is the quotient of the rotation period to the number of blades and thus provides no useful information for crack detection. Based on this reasoning, the mean of the ToA data is removed.

2) The rotation period is a function of rotation speed and therefore the demeaned ToA data need to be normalized with respect to the corresponding speed to eliminate the speed-related effects.

3) A periodic change in ToA could take place if the rotor shaft is bent in operation. The interference signal generated by this bending effect should be analyzed and eliminated from the original signal.

Because of the bending of rotor shaft, the physical axis of the shaft recedes from the geometric rotation axis as shown in Fig. 2.5.1(a). As a result, the virtual plane on which the disc and the blades are located is no longer perpendicular to the geometric rotation axis. The deviation in orientation angle results in an angular oscillation of the aforementioned virtual plane with the period equal to that of a

complete rotation of the shaft. The radial eccentricity of the disc has a negligible effect on ToA whereas the angular deformation γ of shaft is of importance in ToA data analysis. As illustrated in Fig. 2.5.1(b), the blades take an axial displacement Δx due to the angular deformation of shaft:

$$\Delta x = h \sin\gamma = R \sin\theta \ \sin\gamma \tag{2.5.1}$$

where the term $R \sin\gamma$ represents the amplitude of the axial oscillation of blades and does not vary while the rotation speed is constant.

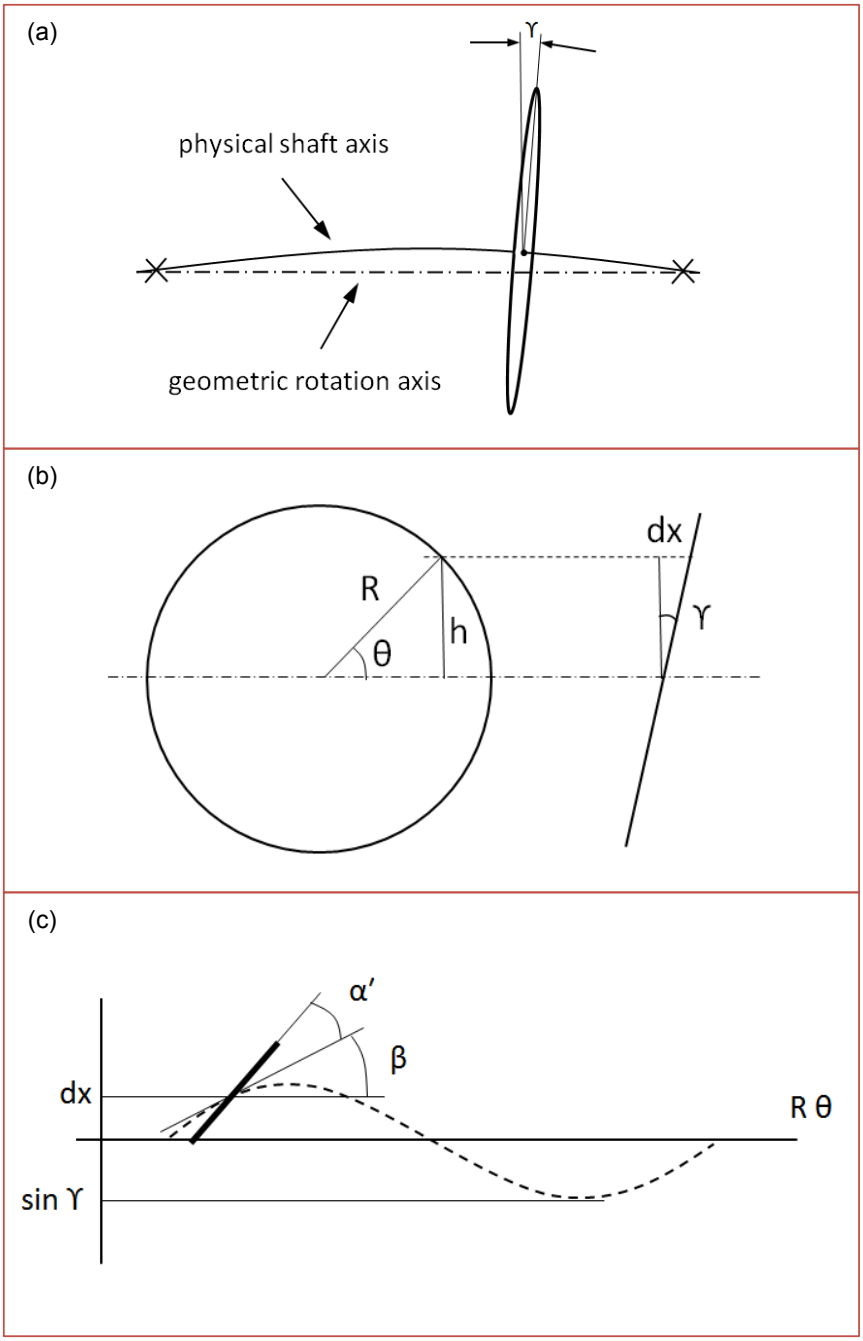

Fig. 2.5.1 Schematic illustrations for rotor bending effects: (a) the angular displacement of the disk on a bent shaft; (b) the consequent axial displacement of the disk periphery; and (c) the variations in blade axial position *Δx* and angle *β* due to axial displacement in disk periphery.

Since the disc plane is angularly oscillating and the blades are located on this plane, the angles of the blades are consequently subject to a periodic change. This periodically-changing angle β is equal to the derivative of the position of the disc periphery with respect to its tangential motion (as illustrated in Fig. 2.5.1(c)):

$$\beta = \frac{d}{d}\left(\frac{\Delta x}{R\theta}\right) = \frac{1}{R}\left(\frac{d\,\Delta x}{d\theta}\right) = \sin\gamma\cos\theta \tag{2.5.2}$$

From (2.3.2.2) and (2.5.1), the deviation in the ToA of the blades caused by the shaft bending effects can be obtained as:

$$\Delta t = \frac{\sin\theta\sin\gamma}{\omega\tan(\alpha' + \beta)} \tag{2.5.3}$$

Considering $\beta \ll \alpha'$, (2.5.3) can be further simplified as:

$$\Delta t = \frac{\sin\gamma}{\omega\ \tan\ \alpha'}\sin\theta \tag{2.5.4}$$

Equation (2.5.4) reveals that the bending of the shaft leads to a deviation in ToA of the blades and this deviation is the first harmonic of the shaft rotation with the amplitude $\sin\gamma/\omega\ \tan\ \alpha'$. Therefore, as in the case of TC, the sinusoidal effect caused by the shaft bending effect should also be removed from the ToA signal in feature extraction. Fig. 2.5.2 shows the magnitude and phase of the computed sinusoidal effects carried by the ToA signal. It can be seen that both the average and normalized standard deviation of these effects do not vary significantly with cycles. These sinusoidal effects are therefore eliminated from the original ToA data.

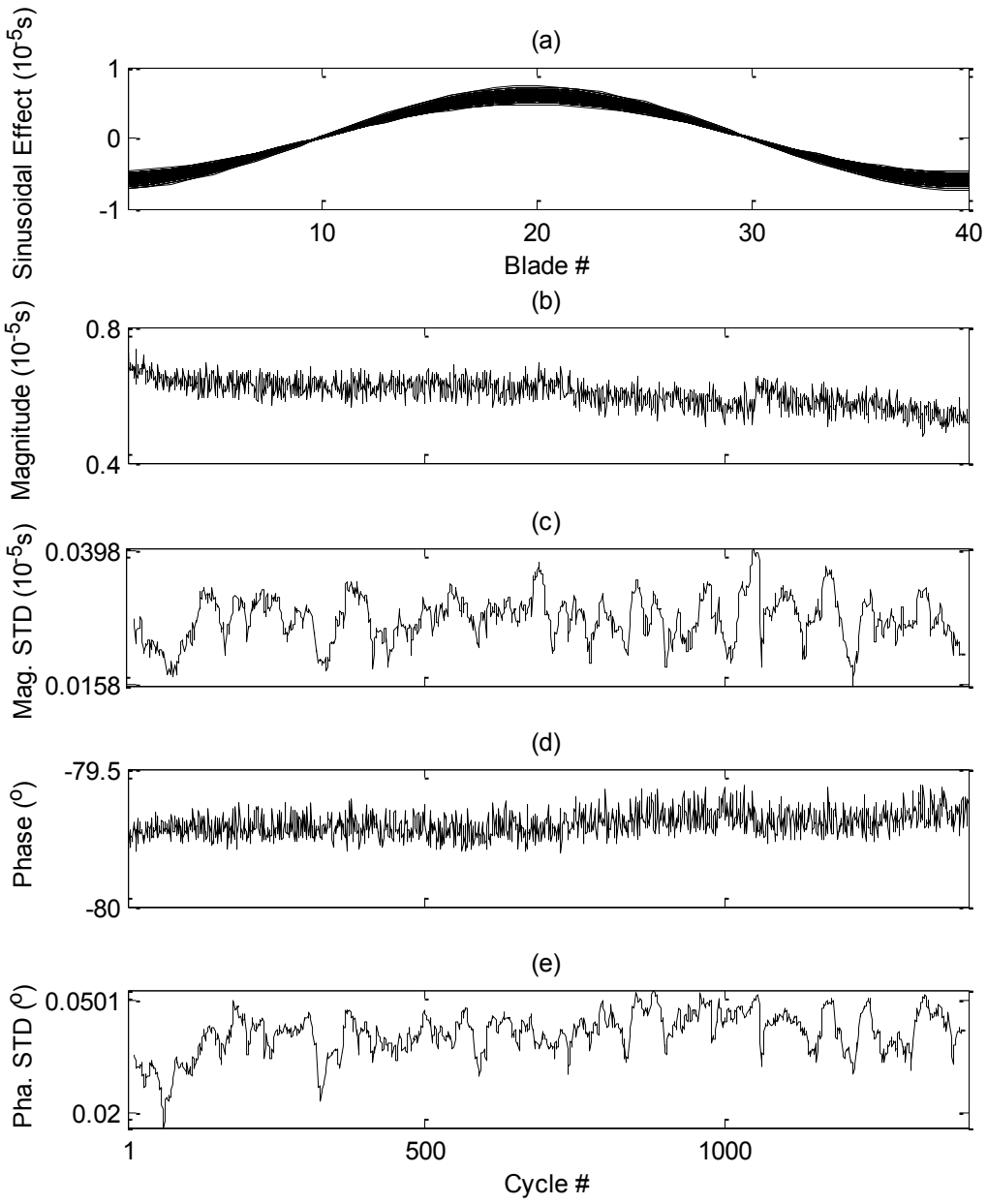

Fig. 2.5.2 The sinusoidal effects carried by the ToA signal and caused by the shaft bending: (a) the sinusoidal effects over 1408 cycles; (b) the magnitude; (c) the localized standard deviation trend of the magnitudes; (d) the phase; and (e) the localized standard deviation trend of the phases.

2.6. SUMMARY

In this chapter, the prepared signals of Tip clearance and Time of Arrival in a an aero engine bladed fan disc are acquired and the physical interpretation is presented. Moreover, a signal preprocessing technique is proposed to remove noise due to temperature changes, disk imbalance, bending effect of the rotating disk shaft and a sinusoidal analysis in applied to observe any changes in the position of rotating disk blades. MATLAB codes are programmed to conduct the suggested TC and ToA signals preprocessing (Appendix A). The results show a stiffness change in bladed disk due to initiating a crack.

CHAPTER THREE

SIGNAL POSTPROCESSING

3.1. INTRODUCTION

As the crack is at its initial stage, the crack-induced signature cannot be observed directly from either the original signal or from the preprocessed one. The preprocessed TC and ToA data need to be further analyzed in this chapter to detect the initiation of the crack and identify the location (i.e., the serial # of the damaged blade) of the crack in the disc. Advanced signal processing has to be conducted next to extract useful features for bladed disk crack detection. Considering that the involved signal is nonstationary in nature, statistical wavelet analysis is suggested in this work for crack related feature extraction. As a second approach for further analysis, a detrended fluctuation analysis (DFA) technique is proposed to fulfill this diagnostic task and make a comparison of the obtained results.

3.2. WAVELET TRANSFORM THEORY

This approach holds remarkable promise in the time-frequency analysis. A wavelet is a waveform of effectively limited duration that has an average value of zero. Mathematically, wavelet transform decomposes a signal into stretched and shifted forms of basis function called a mother wavelet. Local features of signal can be most suitably described with wavelets [38].

3.2.1. A FAMILY OF WAVELETS

Simple, fixed building blocks at different scales and positions are involved in wavelet transform for representing general functions. These building blocks are a family of "wavelet" functions or in short the "wavelets". Mother wavelet is a single fixed function which generates the wavelets, by translation and dilation (scaling) operations [51]. Mother wavelet is defined as a function $\psi(t)$ so that its Fourier transform $\Psi(\omega)$ satisfies [19, 56]:

$$\int_{-\infty}^{+\infty} \frac{|\Psi(\omega)|^2}{\omega} d\omega = C_\psi < +\infty \tag{3.2.1.1}$$

This condition is known as the "admissibility condition" and implies that [47],

$$\int_{-\infty}^{+\infty} \psi(t) dt = 0 \tag{3.2.1.2}$$

To create a family of scaled and shifted versions of the basis wavelet, scaling and translation operations performed on the mother wavelet $\psi(t)$ as equation 3.2.2 where respectively, a is the scaling and b is the translation parameters, and the factor $\frac{1}{\sqrt{|a|}}$ is used to ensure that the energy of the scaled and translated versions are the same as the mother wavelet [56].

$$\psi_{a,b}(t) = \frac{1}{\sqrt{|a|}} \psi\left(\frac{t-b}{a}\right) \tag{3.2.1.3}$$

To obtain different frequency information of the signal to be analyzed, stretching and compressing operations performed on the mother wavelet by changing the scale factor. For achieving the time information of the function to be analyzed, the mother wavelet is shifted along the time axis by varying translation factor. Figure 3.2(a) shows an example of a mother wavelet, the Mexican hat function and the shifted, figure 3.2(d), compressed, figure 3.2(b) and stretched wavelets figure 3.2(c).

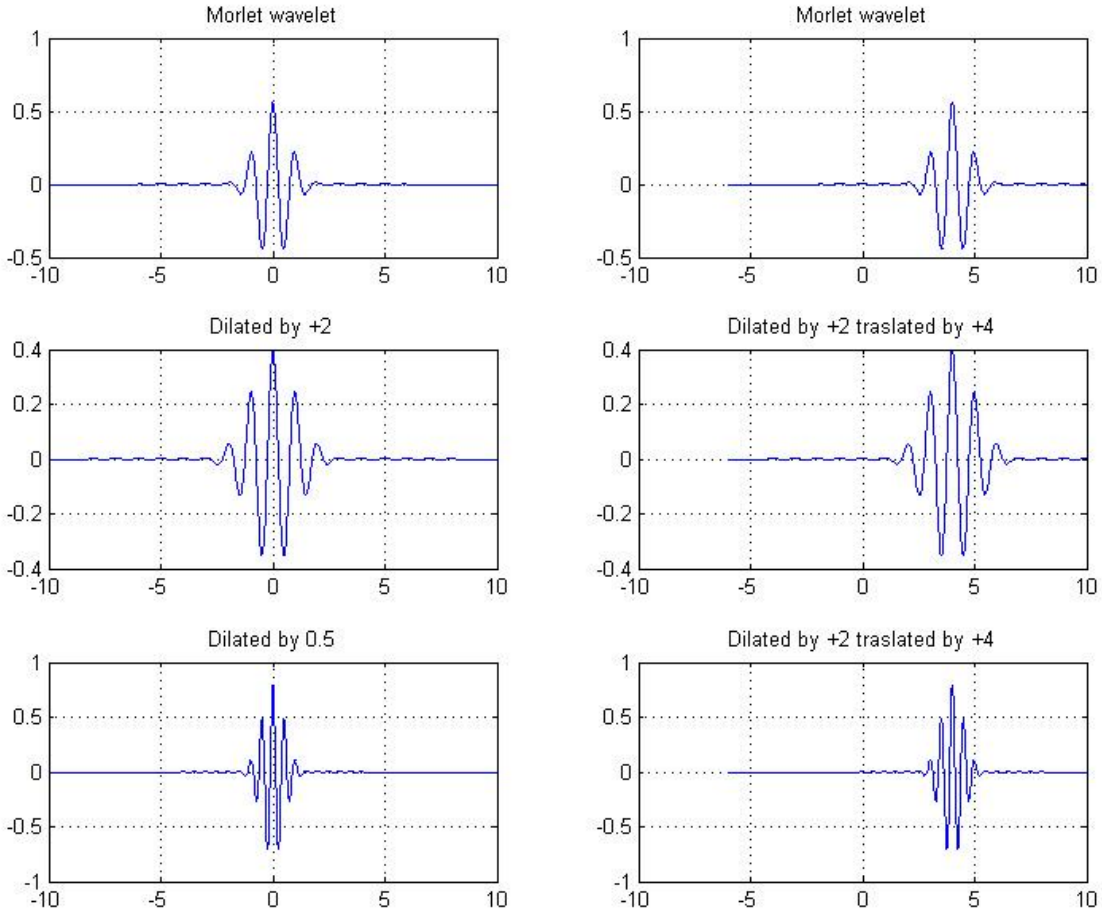

Fig. 3.2 The Morlet mother wavelet and its scaled and translated versions [51].

3.2.2. CONTINUOUS WAVELET TRANSFORM

The mathematical aspects of continuous wavelet transform are similar to those of short-time Fourier transform [18]. Given a mother wavelet function $\psi(t)$, continuous wavelet transform CWT of a function $f(t)$ is defined by:

$$CWT_f(a,b) = \frac{1}{\sqrt{|a|}} \int_{-\infty}^{+\infty} f(t)\psi^*\left(\frac{t-b}{a}\right) dt \qquad a,b \in R, a \neq 0 \tag{3.2.2}$$

where the asterisk denotes the complex conjugate [56]. Consequently, wavelet analysis maps a signal $f(t)$ into a two-dimensional plot. The level at each point is a function of time and scale instead of time and frequency. The scale in itself is related to frequency, as the frequency is inversely proportional to a scale factor. High scales correspond to the stretches wavelets and low scales to compressed wavelets. Thus, wavelet transform is capable of zooming-in on short-lived high frequency phenomena, and zooming out on long-lived low frequency phenomena. Low scales describe the rapidly changing details and high scales give the slowly changing coarse features.

Unlike Fourier method which uses a single analysis window function, the wavelet transform can use short windows at high frequencies and long windows at low frequencies. This leads to that the ratio of frequency resolution to the center frequency remains constant. Wavelet analysis is thus a constant relative bandwidth analysis unlike Fourier transform that is a constant bandwidth analysis [51]. This is one the main advantages of wavelet transform over short-time Fourier transform.

Roughly speaking, a wavelet transform coefficient, $CWT_f(a, b)$, at a particular scale and translation represents how well the function $f(t)$, and the scaled and shifted wavelet $\psi_{(a,b)}(t)$ match. If they are similar to each other, then this coefficient will be large in magnitude.

3.3. WAVELET ANALYSIS FOR CRACK IDENTIFICATION

As one of the most effective solutions for picking up health condition related signatures in the field of structural health monitoring, wavelet transform essentially decomposes a signal into wavelet coefficients through a convolution process. Stress cycling or steady state operation at high temperatures results in damage evolution in the form of wear and internal microstructural damage which initiate crack nucleation leading to small change in stiffness of assembly [58].

Further stressing of the disk produces changes in the material characteristics and stiffness, affecting the tip clearance, time of arrival of the individual blades, magnitude and phase of the displacements [58]. The subtle changes in the signature arising as a result of changes in the stiffness could potentially be picked from the test data. The method is known to be effective in capturing minute nonstationary changes that are not readily discernible in the traditional FFT-based frequency analysis.

The choice of an appropriate mother wavelet depends on the signal properties and the purpose of the analysis. In this work, the interest is to obtain the minute changes in the tip clearance and time-of-arrival signal that are induced by a localized crack in a rotating disk. Through some initial testing, the Daubechies db4 wavelet is eventually selected as the mother wavelet. Given a time-domain signal $x(t)$, the wavelet coefficients can be determined by,

$$\mathrm{WT_x(t,s)} = \int_{-\infty}^{+\infty} \mathrm{x(\tau)\sqrt{s}\, w^*\big(-s(t-\tau)\big)d\tau} \tag{3.3.1}$$

Where $w^*(t)$ denotes the complex conjugation of mother wavelet function w(t); s and t are the scale and time variables, respectively, which produce dilation and translation [56]. The wavelet transform is conducted on the preprocessed tip clearance and time-of-arrival signal for each blade over 1408 data-recording cycles using a MATLAB code in Appendix A.

3.3.1. Statistical Wavelet Analysis Based on the Blades

To reveal the changing characteristics of the bladed disk, further statistical analysis applied on the obtained wavelet coefficients. Based on the previous experience of the investigator, the two statistical parameters, standard deviation and kurtosis (fourth moment) of the levels of the wavelet coefficients were selected [38].

First approach is to extract the changing feature based on the blades. This leads to identifying the location of crack in respect to the serial number of blade. The standard deviation and kurtosis of the obtained wavelet coefficients for each blade corresponding to each wavelet scale is obtained and presented in Fig. 3.3.1.1, Fig. 3.3.1.2 and Fig. 3.3.1.3. It is seen that the blades (blade # 32 and 33) with an incipient crack developing underneath give the highest values of the standard deviation of the wavelet coefficients when the scale is higher.

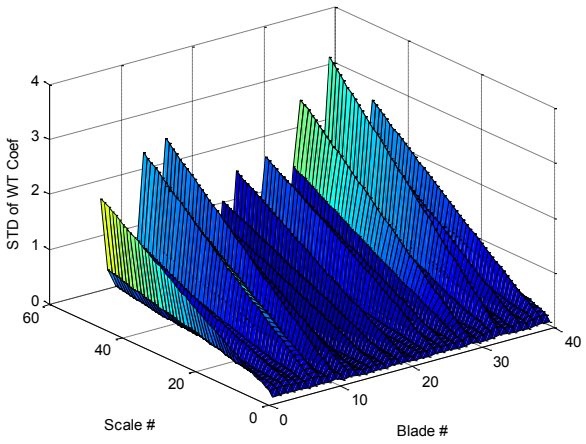

Fig. 3.3.1.1 The standard deviation of the wavelet coefficients over 48 scales for 40 blades based on the Time-of-arrival signal.

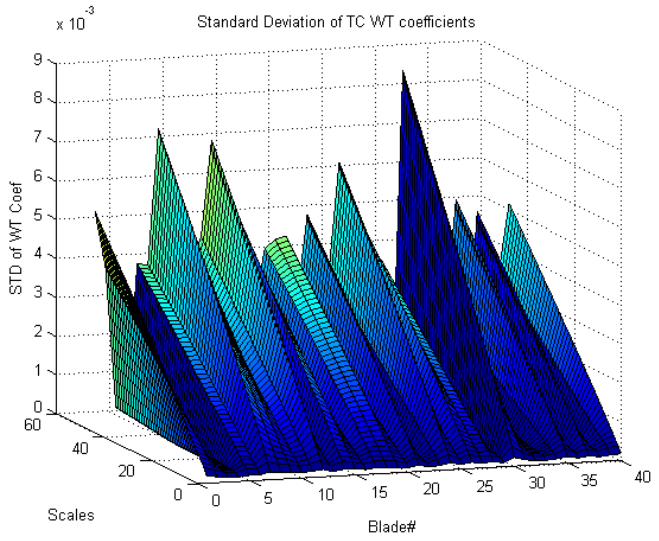

Fig. 3.3.1.2 The standard deviation of the wavelet coefficients over 48 scales for 40 blades based on the Tip Clearance signal.

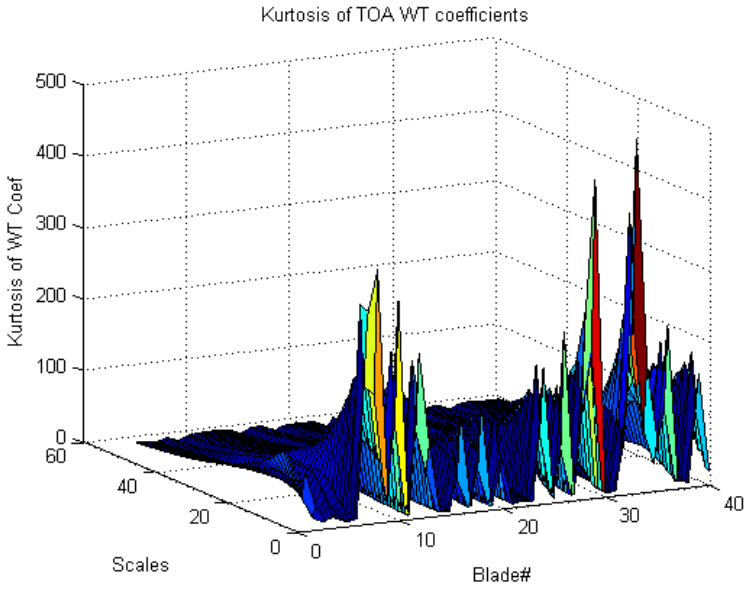

Fig. 3.3.1.3 The Kurtosis of the wavelet coefficients over 48 scales for 40 blades based on the Time of arrival signal.

3.3.2. STATISTICAL WAVELET ANALYSIS BASED ON THE LIFE CYCLES

The next step in the analysis was to extract the features of the map at varying stages of the life cycle of the disk. By extracting changing features from the WT coefficient analysis based on cycles, crack initition in the life cycle of tested bladed disk can be achieved. The standard deviation and kurtosis of the obtained wavelet coefficients for each blade corresponding to each wavelet scale is calculated and presented in Fig. 3.3.2.1 - 3.3.2.4.

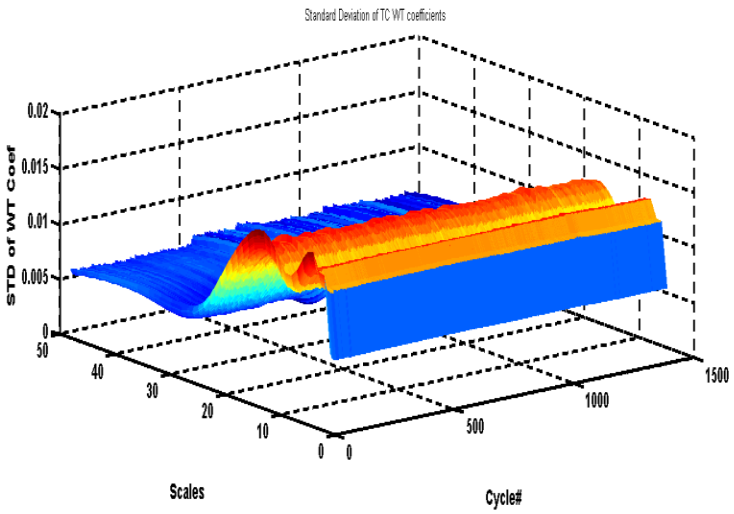

Fig. 3.3.2.1 The STD of the wavelet coefficients over 48 scales for 1408 cycles based on the Tip Clearance signal.

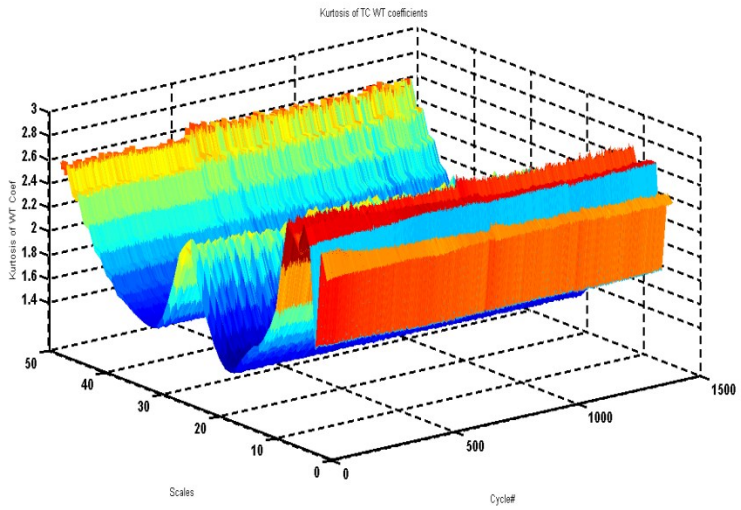

Fig. 3.3.2.2 The Kurtosis of the wavelet coefficients over 48 scales for 1408 cycles based on the Tip Clearance signal.

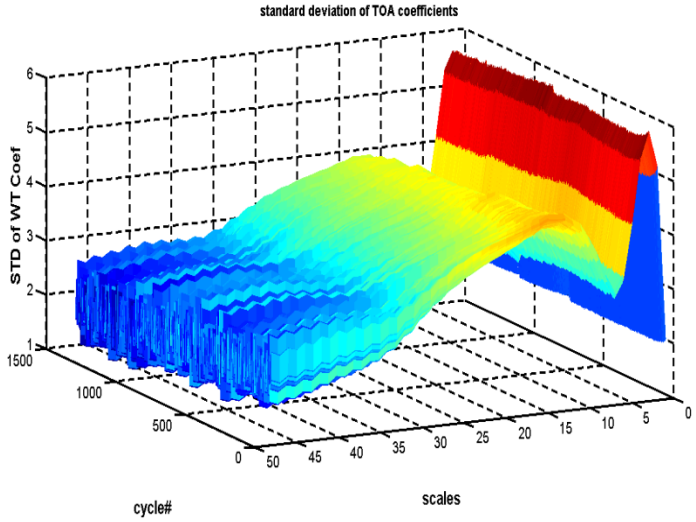

Fig. 3.3.2.3 The STD of the wavelet coefficients over 48 scales for 1408 cycles based on the Time of Arrival signal.

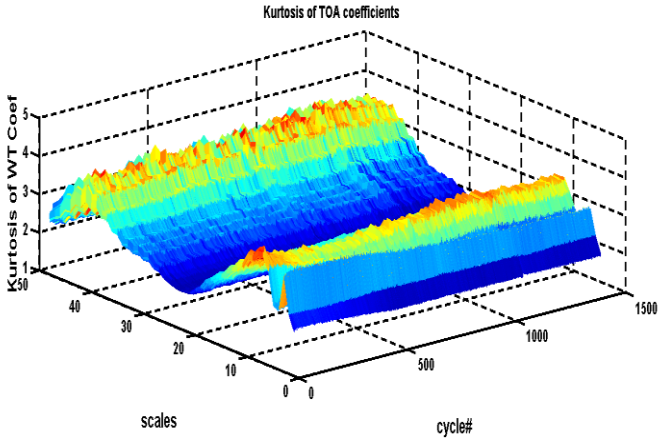

Fig. 3.3.2.4 The Kurtosis of the wavelet coefficients over 48 scales for 1408 cycles based on the Time of Arrival signal.

This useful information could be potentially regarded as an indicator for bladed disk crack detection. However, for more reliable crack detection, more representative features need to be extracted from various types of signal sources and the contributions of these features could be integrated in a decision-making process [54]. In the next section, a statistical analysis is proposed to validate the results obtained from wavelet analysis based on blades.

3.4. DETRENDED FLUCTUATION ANALYSIS FOR CRACK LOCATION IDENTIFICATION

The DFA was introduced in 1994 as a fractal scaling method intended for detecting the autocorrelations in noisy and nonstationary time series [59]. The method has found sound applications in a wide range of science, medical, and engineering fields, including physiology, geophysics, finance, cardiac dynamics, bioinformatics, ecology and many more [60], but none in machine fault detection before 2011. The author's research group presented the first adaption of the DFA technique for bearing fault

detection in 2011 and the research results showed that the DFA is effective in discriminating bearing health conditions [4]. The current work intends to extend its application to bladed disk crack detection.

Given a noisy and nonstationary time series $x(i), i = 1, \cdots, N$, the standard DFA technique starts by computing the DC component of the time series:

$$\bar{x} = (1/N) \sum_{i=1}^{N} x(i) \tag{3.4.1}$$

An integrated time series $y(j),\ j = 1, \cdots, N$, is then obtained:

$$y(j) = \sum_{i=1}^{j} [x(i) - \bar{x}] \tag{3.4.2}$$

The integrated time series $y(j)$ is divided into N/n non-overlapping boxes, each containing n points of data. Define the "local trend" in each box to be the ordinate of a linear least-square fit for the data sequence in each box. This fit, denoted by $y_{fit}(j)$, is then employed to obtain the detrended fluctuation function (i.e., the detrended walk):

$$Y(j) = y(j) - y_{fit}(j) \tag{3.4.3}$$

For a given box size n (i.e. the scale), calculate the variance about the detrended walk:

$$F^2(n) = \frac{1}{\mathrm{N}}\sum_{1}^{\mathrm{N}}[\mathrm{Y(j)}]^2 \tag{3.4.4}$$

Repeat the above procedure for a broad range of box sizes to obtain the relationship between $F(n)$ and n. By analyzing this relationship, it is possible to verify the presence of fractal characteristics in the signal. A power-law relation between $F(n)$ and n indicates the presence of scaling:

$$F(n) \sim n^{\alpha} \tag{3.4.5}$$

where the parameter α (alpha) is the scaling exponent that corresponds to the slope of a specific DFA curve relating $\log^{\mathrm{F(n)}}$ to $\log^{\mathrm{n}}$. The logarithmic base has no effect on the power α. This scaling exponent represents the correlation properties of the signal. In the case of having only short-range correlations (or no correlations at all) the detrended walk profile displays properties of a standard random walk with $\alpha = 0.5$. On the other hand, if $\alpha < 0.5$, the correlations in the signal are anti-persistent, i.e., negative correlation; if $\alpha > 0.5$, the correlations in the signal are persistent, i.e., positive correlation. The value $\alpha \to 0$ is indicative of a behavior with tendency to be harmonic dynamics.

The DFA offers the advantage over the traditional signal analysis methods in that it can deal with nonstationary signals like TC or ToA data, and also its application does not rely on the selection of mother functions as the wavelet transform does [20]. In

this work, the DFA is applied to characterize the dynamics of the rotating bladed disk. The underlying idea behind the application is to investigate the scaling properties of the entire signal distribution to detect the existence of the correlations embedded in the nonstationary blade-passage signals associated with different disk health conditions. Fig. 3.4.1(a) shows the generated scaling exponent trend from the preprocessed TC signal. It can be clearly seen that the blades (blade #: 32 and 33) with an incipient crack underneath exhibit much larger alphas than the rest of the blades in the disk. Meanwhile, Fig. 3.4.1(b) shows the generated scaling exponent trend from the preprocessed ToA signal. It can be observed that the damaged blades still take on the highest alphas, although not as remarkable as the ones derived from the preprocessed TC signal due to the fact that the spin rig test does not involve the hot gas flow. From these testing results, it is clear that the DFA technique does not make assumptions about signal stationarity, thus presenting an effective and practical approach for bladed disk crack detection. The power-law characteristic possesses a good potential as a statistic monitoring index to distinguish the damaged bladed disk condition from the healthy one.

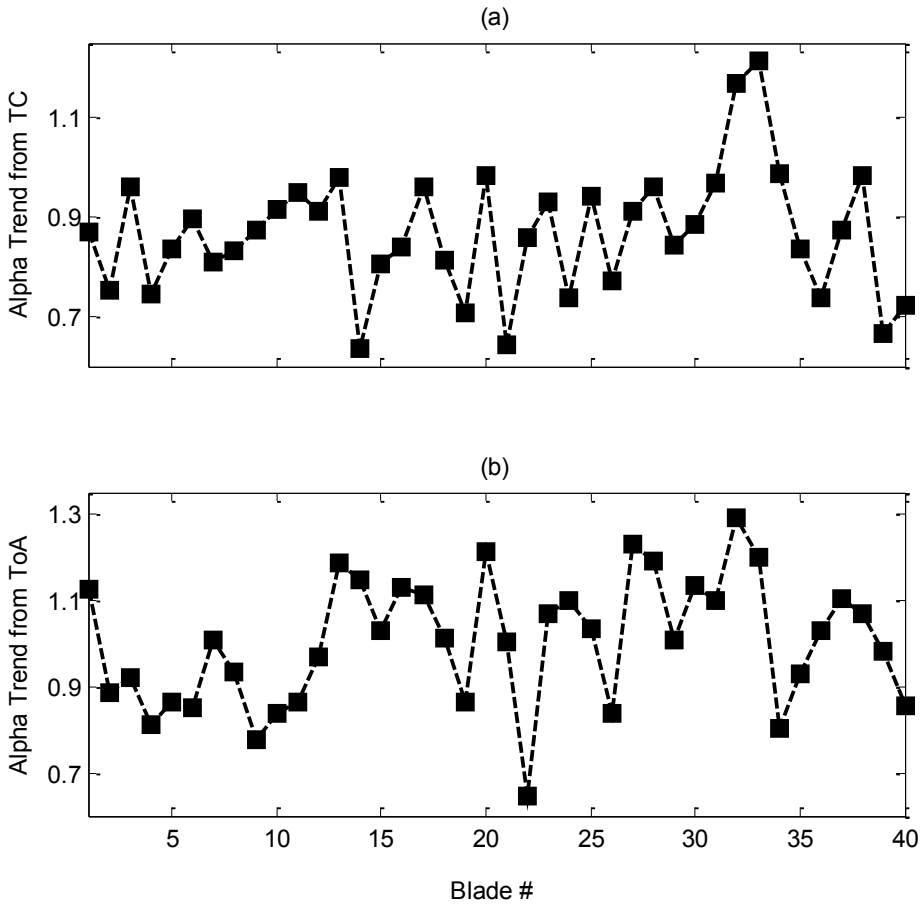

Fig. 3.4.1 The alpha trend derived from the DFA for bladed disk crack detection based on: (a) the preprocessed TC data; and (b) the preprocessed ToA data.

3.5. SUMMERY

Feature extraction is conducted on the blade passage signals through two stages of signal processing as elaborated in this chapter. At first stage, the wavelet analysis is expected to reveal the changing characteristics of the disk. In this phase of the analysis, the effort was focused on defining the methods and demonstrating the feasibility of the wavelet analysis in tracking down the varying features of the disk

during its spin rig testing life cycle.

Secondly, signal post-processing conducted to identify the crack location through the proposed detrended fluctuation analysis (DFA). Traditional approaches such as the power-spectrum and correlation analysis are not suited to accurately quantify correlations in nonstationary signals.

CHAPTER FOUR

CONCLUSIONS AND RECOMMENDATIONS

4.1 CONCLUSIONS

A novel technique is proposed in this work for bladed disk crack diagnostics through two sequential stages: 1) signal preprocessing to reduce or eliminate the noises induced by various known factors other than defects. Physical modeling is established in this process to characterize these noises. The crack initiation time can be determined by using the suggested localized standard deviation of the sinusoidal effects caused by the rotor imbalance. The physical model for the sinusoidal effect caused by the rotor bending is established. This interfering effect is then removed from the original time-of-arrival signal at the signal preprocessing stage to enhance the signal-to-noise ratio.

The statistical wavelet analysis is then conducted on the preprocessed time-of-arrival data to identify the crack location in the disk. Experimental results show that the suggested technique is capable of providing useful indicative information for locating the incipient crack that occurs in the bladed disk.

The DFA is a scaling analysis method providing a quantitative parameter, i.e., the scaling exponent, to represent the correlation properties of a signal.

The proposed technique distinguishes the bladed disk cracking condition by investigating the power-law characteristics of the blade passage signals. The viability of the proposed technique is verified through the experimental data set.

The testing results have demonstrated that the developed techniques are an effective approach for identifying and locating the incipient crack that occurs at the root of a bladed disk.

4.2 FUTURE WORKS

The present work is done based on the Tip clearance and Time of arrival data of an aero-engine bladed fan disc. The available data may not allow more comprehensive analysis. If additional data are available in future, further studies in the following directions could be worth exploring:

a. Identifying the various stages of damage evolution during its life cycle by extracting other effective parameters except standard deviation and kurtosis from wavelet map.
b. Different wavelets be examined to develop efficient algorithms to identify the stress levels, crack initiation, crack growth to its final rupture.
c. The characteristics of the modulation change during the life cycle of the disk spin rig test should be examined.

REFERENCES

[1]. A. KS Jardine, D. Lin, and D. Banjevic. "A review on machinery diagnostics and prognostics implementing condition-based maintenance." Mechanical systems and signal processing 20.7 (2006): 1483-1510.

[2]. Aninda Bhattacharya , et al. "System to monitor blade health in axial flow compressors." Prognostics and Health Management (PHM), 2011 IEEE Conference on. IEEE, 2011.

[3]. M. J. Schulz, and M. J. Sundaresan. "Smart Sensor System for Structural Condition Monitoring of Wind Turbines." (2006).

[4]. J. Liu, "Detrended fluctuation analysis of vibration signals for bearing fault detection", Proceedings of the IEEE International Conference on Prognostics and Health Management (PHM), Denver, Colorado, USA, June 2011.

[5]. M. P. Hanson, A. J. Meyer, and S. S. Manson. "A Method of Evaluating Loose Blade Mounting as a Means of Suppressing Turbine and Compressor Blade Vibration." Proc. Soc. Exptl. Stress Anal. Vol. 10. No. 2. 1953.

[6]. J. Kenyon, J H Griffin, and DM Feiner, "Maximum bladed disk forced response from distortion of a structural mode." Journal of Turbomachinery(Transactions of the ASME) 125.2 (2003): 352-363.

[7]. L. Gelman, P. White, and J. Hammond, "Fatigue crack diagnostics: a comparison of the use of the complex bicoherence and its magnitude," Mechanical Systems and Signal Processing, vol. 19, pp. 913-918, 2005.

[8]. P. C. Ivey, K. R. Grant, and C. Lawson. "Tip Timing Techniques For Turbomachinery HCF Condition Monitoring." the 16 th Symposium on Measuring Techniques in Transonic and Supersonic Flow in Cascades and Turbomachines, Cambridge, UK. 2002.

[9]. R. F. Orsagh, and M.J. Roemer. Examination of Successful Modal Analysis Techniques Used for Bladed-Disk Assemblies. Impact Technologies LLC Rochester NY, 2002.

[10]. M. Metwally, W. Tabakoff, and A. Hamed. "Blade erosion in automotive gas turbine engine." Journal of engineering for gas turbines and power 117.CONF-930502-- (1995).

[11]. M. S. Lebold, S. Mitchell, et al. "Using torsional vibration analysis as a synergistic method for crack detection in rotating equipment." Aerospace Conference, 2004. Proceedings. 2004 IEEE. Vol. 6. IEEE, 2004.

[12]. M. Zielinski, and G. Ziller. "Noncontact Crack Detection on Compressor Rotor Blades to Prevent Further Damage after HCF-Failure." NATO/PFP (RTO-MP-AVT-121) 19 (2005): 1-10.

[13]. X. Fang, J. Tang, E. Jordan, and K.D. Murphy, "Crack induced vibration localization in simplified bladed-disk structures." Journal of sound and vibration 291.1 (2006): 395-418.

[14]. T. Nicholas, “High cycle fatigue life management in gas turbine engines”, NATO Research and Technology Organization, RTO-MP-17, Report No.: AC/323(AVT)TP/7, 1999.

[15]. C. Ruiz, P.H.B. Boddington and K.C. Chen, “An investigation of fatigue and fretting in a dovetail joint”, Experimental Mechanics, vol. 24, no. 3, pp. 208-217, 1984.

[16]. D. Kumar, J. Crocker, J. Knezevic, M. El-Haram, “Reliability maintenance and logistic support – A life cycle aproach”, Springer, edition 1, pp. 182-183, 2000.

[17]. I. Soltani Bozchalooi, and M. Liang. "A smoothness index-guided approach to wavelet parameter selection in signal de-noising and fault detection." Journal of Sound and Vibration 308.1 (2007): 246-267.

[18]. M. Liang, and I. Soltani Bozchalooi, "An energy operator approach to joint application of amplitude and frequency-demodulations for bearing

fault detection." Mechanical Systems and Signal Processing 24.5 (2010): 1473-1494.

[19]. I. Soltani Bozchalooi, and M. Liang, "A joint resonance frequency estimation and in-band noise reduction method for enhancing the detectability of bearing fault signals." Mechanical Systems and Signal Processing 22.4 (2008): 915-933.

[20]. H. Hong, and M. Liang, "Separation of fault features from a single-channel mechanical signal mixture using wavelet decomposition.", Mechanical systems and signal processing 21.5 (2007): 2025-2040.

[21]. B.O. Al-Bedour, L. Ghouti, S.A, Adewusi, Y. AL-Nassar and M. Abdlsamad, “Experiments on the extraction of blade vibration signature from the shaft torsional vibration signals”, Journal of Quality in Maintenance Engineering, Iss: 2, pp. 144-159,2003.

[22]. Li, C. J., and J. H. Lee. "Non-contact rotating beam crack size estimation from vibro-acoustic signals." Measurement Science and Technology 17.6 (2006): 1529.

[23]. T. Kawashima, H. Iinuma and N. Minagawa, “Optical semiconductor blade vibration monitoring system for gas turbine engine”, Proceedings of Instrumentation and Measurement Technology Conference, 10th Anniversary, pp. 601-604, 1994.

[24]. D. Mba, , Rao, B. K. N. Raj,“Development of Acoustic Emission Technology for Condition Monitoring and Diagnosis of Rotating Machines: Bearings, Pumps, Gearboxes, Engines, and Rotating Structures”, The Shock and Vibration Digest, 2006, Vol 38(1), pp3-16

[25]. X.H. Wang, C.M. Zhu, H.L. Mao , and Z.F. Huang, "Wavelet packet analysis for the propagation of acoustic emission signals across turbine runners." NDT & E International 42.1 (2009): 42-46.

[26]. A. Von Flotow, "Apparatus and method for predicting failures of spinning disks in turbo-machinery." U.S. Patent No. 6,785,635. 31 Aug. 2004.

[27]. A. von Flotow, M. Mercadal and P. Tappert, “Health monitoring and prognostics of blades and disks with blade tip sensors”, Proceedings of IEEE Aerospace Conference, vol. 6, pp. 433-440, 2000.

[28]. A. Steiner, "Techniques for blade tip clearance measurements with capacitive probes." Measurement Science and Technology 11.7 (2000): 865.

[29]. A. von Flotow and M.J. Drumm, “High temperature, through the case, eddy current blade tip sensors,” Hood Technology, unpublished.

[30]. G. Zenzinger, J. Bamberg, M. Dumm, and P. Nutz, "Crack detection using eddytherm." AIP Conference Proceedings. Vol. 760. 2005.

[31]. P. Tappert, A. von Flotow and M. Mercadal, “Autonomous PHM with blade-tip-sensors: algorithms and seeded fault experience” Proceedings of IEEE Aerospace Conference, vol. 7, pp. 7-3295, 2001.

[32]. M. Zielinski and G. Ziller, “Noncontact Blade Vibration Measurement System for Aero Engine Application”, Proceedings of 17th International Symposium on Airbreathing Engines, pp. 4-9, 2005.

[33]. M. P. Norton, and D. G. Karczub. Fundamentals of noise and vibration analysis for engineers. Cambridge university press, 2003.

[34]. N. Tandon, and A. Choudhury, "A review of vibration and acoustic measurement methods for the detection of defects in rolling element bearings." Tribology International 32.8 (1999): 469-480.

[35]. W. Q Jeffries., J. A. Chambers, and D. G. Infield, "Experience with bicoherence of electrical power for condition monitoring of wind turbine blades." Vision, Image and Signal Processing, IEE Proceedings-. Vol. 145. No. 3. IET, 1998.

[36]. C. Wang and R.X. Gao, “Wavelet transform with spectral post-processing for enhanced feature extraction,” IEEE Transactions on Instrumentation and Measurement, vol. 52, no. 4, pp. 1296-1301, 2003.

[37]. B. Zhang, C. Sconyers, C. Byington, R. Patrick, M.E. Orchard, and G. Vachtsevanos, “A probabilistic fault detection approach: application to bearing fault detection,” IEEE Transactions on Industrial Electronics, vol. 58, pp. 2011-2018, 2011.

[38]. J. Liu, W. Wang, and F. Golnaraghi, “An enhanced diagnostic scheme for bearing condition monitoring,” IEEE Transactions on Instrumentation and Measurement, vol. 59, pp. 309-321, 2010.

[39]. T. Kaewkongka, , et al. "A comparative study of short time Fourier transform and continuous wavelet transform for bearing condition monitoring." International Journal of COMADEM 6.1 (2003): 41-48.

[40]. B. S. Kim, et al. ,"A comparative study on damage detection in speed-up and coast-down process of grinding spindle-typed rotor-bearing system.", Journal of materials processing technology 187 (2007): 30-36.

[41]. T. Boutros, and M. Liang. "Mechanical fault detection using fuzzy index fusion." International Journal of Machine Tools and Manufacture 47.11 (2007): 1702-1714.

[42]. J. Antoni, and R. B. Randall, "The spectral kurtosis: application to the vibratory surveillance and diagnostics of rotating machines.", Mechanical Systems and Signal Processing 20.2 (2006): 308-331.

[43]. N. Sawalhi, and R. B. Randall, "Spectral kurtosis optimization for rolling element bearings.", Signal Processing and Its Applications, 2005. Proceedings of the Eighth International Symposium on. Vol. 2. IEEE, 2005.

[44]. H. Hong, and M. Liang. "Fault severity assessment for rolling element bearings using the Lempel–Ziv complexity and continuous wavelet transform." Journal of sound and vibration 320.1 (2009): 452-468.

[45]. R. B. Randall, J. Antoni, and S. Chobsaard. "The relationship between spectral correlation and envelope analysis in the diagnostics of bearing faults and other cyclostationary machine signals." Mechanical Systems and Signal Processing 15.5 (2001): 945-962.

[46]. M. Cavacece, and A. Introini. "Analysis of damage of ball bearings of aeronautical transmissions by auto-power spectrum and cross-power spectrum." Journal of vibration and acoustics 124.2 (2002): 180-185.

[47]. J. Liu, W. Wang, and F. Golnaraghi, “An extended wavelet spectrum for bearing fault diagnostics”, IEEE Transactions on Instrumentation and Measurement, vol. 57, pp. 2801-2812, 2008.

[48]. H. Zheng, Z. Li, and X. Chen. "Gear fault diagnosis based on continuous wavelet transform." Mechanical systems and signal processing 16.2 (2002): 447-457.

[49]. Ruqiang Yan, and Robert X. Gao. "Energy-based feature extraction for defect diagnosis in rotary machines." Instrumentation and Measurement, IEEE Transactions on 58.9 (2009): 3130-3139.

[50]. Wilson Q. Wang, Fathy Ismail, and M. Farid Golnaraghi. "Assessment of gear damage monitoring techniques using vibration measurements." Mechanical Systems and Signal Processing 15.5 (2001): 905-922.

[51]. X. D. Dai, B. Joseph, and R. L. Motard, “Introduction to wavelet transform and time-frequency analysis.”, Wavelet Applications in Chemical Engineering, (1994) ,1-32.

[52]. X. Fan, M. Liang, T. H Yeap, and B. Kind, "A joint wavelet lifting and independent component analysis approach to fault detection of rolling element bearings." Smart Materials and Structures 16.5 (2007): 1973-1987.

[53]. X. H. Wang, C. M. Zhu, H. L. Mao, and, Z. F. Huang, (2009). Wavelet packet analysis for the propagation of acoustic emission signals across turbine runners. NDT & E International, 42(1), 42-46.

[54]. J. Liu, W. Wang, and F. Golnaraghi, “An enhanced diagnostic scheme for bearing condition monitoring”, IEEE Transactions on Instrumentation and Measurement, vol. 59, pp. 309-321, 2010.

[55]. P. Procházka, F. Vaněk, “Contactless diagnostics of turbine blade vibration and damage” ,9th International Conference on Damage Assessment of Structures (DAMAS 2011), Journal of Physics: Conference Series, vol. 305, 2011.

[56]. G. Strang and T. Nguyen, Wavelets and Filter Banks, Wellesley, MA: Wellesley-Cambridge Press, 1996.

[57]. W. Beres, J. Mackwood, Spin rig faclity, Structure and Material performance, NRC Institute for aerospace research, 2006.

[58]. D. Knappett and J. Garcia, “Blade tip timing and strain gauge correlation on compressor blades”, Proceedings of the Institution of Mechanical Engineers, Part G: Journal of Aerospace Engineering, vol. 222, pp. 497-506, 2008.

[59]. C. K. Peng, S. V. Buldyrev, S. Havlin, M. Simons, H.E. Stanley, and A.L. Goldberger, “Mosaic organization of DNA nucleotides,” Physical Review E, vol. 49, pp. 1685-1689, 1994.

[60]. L. Vela-Martinez, J.C. Jauregui-Correa, E. Rodriguez, and J. Alvarez-Ramirez, “Using detrended fluctuation analysis to monitor chattering in cutter tool machines,” International Journal of Machine Tools & Manufacture, vol. 50, pp. 651-657, 2010.

APPENDICES

APPENDIX A

```
%%%%%%%%%%%%%%% first harmonic fourier coef's %%%%%%%%%%%%%%%%%%%

clc;clear all;
tc=xlsread('tc_modified');
TC_avg_blade=(mean(tc,2));      % mean value of a row(cycle) of TC
TC_comp=tc-repmat(TC_avg_blade,1,40);

a=zeros(1408,1);
b=zeros(1408,1);
for ii=1:1408
        for jj=1:40
            a(ii)=a(ii)+(TC_comp(ii,jj)*cos((jj-1)*pi/20));
            b(ii)=b(ii)+(TC_comp(ii,jj)*sin((jj-1)*pi/20));
        end
        a(ii)=a(ii)/20;
        b(ii)=b(ii)/20;
end

%% %%%%%%%%%%% first harmonic sine wave calculation %%%%%%%%%%%%%%%%%
fourier=zeros(1408,40);
TC_dt_comp=zeros(1408,40);       % sinusoidal effect is removed
for ii=1:1408
    for jj=1:40
        fourier(ii,jj)=a(ii)*cos((jj-1)*pi/20)+b(ii)*sin((jj-1)*pi/20);
        TC_dt_comp(ii,jj)=TC_comp(ii,jj)-fourier(ii,jj);
    end
end
%% %%%%%%%%%%% phase diffrence due to imbalancy %%%%%%%%%%%%%%%%%%%

% for index=1:1408
%    hold on
%    plot(fourier(index,:))
% end
```

```
%% ######### wavelet coefficient based on blades ##########################

TC_COEF=zeros(48,1408,40);
for index=1:40
    TC_V=TC_dt_comp(:,index)';
    TC_COEF(:,:,index)=cwt(TC_V,1:48,'db4');

end

%% ################## standard deviation based on blades ##################

TC_Sd=zeros(48,40);
for ii=1:40
    TC_Sd(:,ii)=std(TC_COEF(:,:,ii),0,2);
end
figure(3);
surf(TC_Sd);grid on;title('Standard Deviation of TC WT coefficients');
ylabel('Scales')
xlabel('Blade#')
zlabel('STD of WT Coef')

%% ############ Kurtosis of WT Coef based on the blades ###############

TC_kurtosis=zeros(48,40);
for ii=1:40
    TC_kurtosis(:,ii)=kurtosis(TC_COEF(:,:,ii),0,2);
end
figure(4);
surf(TC_kurtosis);grid on;title('Kurtosis of TC WT coefficients');
ylabel('Scales')
xlabel('Blade#')
zlabel('Kurtosis of WT Coef')

%% ################## wavelet coefficient based on cycles ###############
```

```
TC_COEF=zeros(48,40,1408);
for index=1:1408
    TC_V=TC_comp(index,:);
    TC_COEF(:,:,index)=cwt(TC_V,1:48,'db4');
end

%% %%%%%%%%%%%%  standard deviation based on cycles %%%%%%%%%%%%%%%%%%

TC_Sd=zeros(48,1408);
for ii=1:1408
    TC_Sd(:,ii)=std(TC_COEF(:,:,ii),0,2);
end

figure(3)
surf(TC_Sd,'EdgeColor','none');grid on;title('Standard Deviation of TC
WT coefficients','fontsize',14,'fontweight','bold');
ylabel('Scales','fontsize',16,'fontweight','bold')
xlabel('Cycle#','fontsize',16,'fontweight','bold')
zlabel('STD of WT Coef','fontsize',16,'fontweight','bold')

%% %%%%%%%%%%%%  Kurtosis based on cycles %%%%%%%%%%%%%%%%%%%%%%%%

TC_kurtosis=zeros(48,1408);
for ii=1:1408
    TC_kurtosis(:,ii)=kurtosis(TC_COEF(:,:,ii),0,2);
end

figure(4)
surf(TC_kurtosis,'EdgeColor','none');grid on;title('Kurtosis of TC WT
coefficients');
ylabel('Scales','fontsize',14,'fontweight','bold')
xlabel('Cycle#','fontsize',14,'fontweight','bold')
zlabel('Kurtosis of WT Coef','fontsize',14,'fontweight','bold')


%% %%%%%%%%%%%% first harmonic fourier coef's %%%%%%%%%%%%%%%%%%
```

```
clc;%clear all;
toa=xlsread('TOA_modified');
toa_avg_blade=(mean(toa,2));      % mean value of a row(cycle) of toa
toa_comp=toa-repmat(toa_avg_blade,1,40);

a=zeros(1408,1);
b=zeros(1408,1);
for ii=1:1408
        for jj=1:40
            a(ii)=a(ii)+(toa_comp(ii,jj)*cos((jj-1)*pi/20));
            b(ii)=b(ii)+(toa_comp(ii,jj)*sin((jj-1)*pi/20));
        end
        a(ii)=a(ii)/20;
        b(ii)=b(ii)/20;
end

%% %%%%%%%%%%%%%%%% first harmonic sine wave calculation %%%%%%%%%%

fourier=zeros(1408,40);
toa_dt_comp=zeros(1408,40);       % sinusoidal effect is removed
for ii=1:1408
    for jj=1:40
        fourier(ii,jj)=a(ii)*cos((jj-1)*pi/20)+b(ii)*sin((jj-1)*pi/20);
        toa_dt_comp(ii,jj)=toa_comp(ii,jj)-fourier(ii,jj);
    end
end

%% %%%%%%%%%%% wavelet coefficient based on the blades %%%%%%%%%%%%%%

toa_COEF=zeros(48,1408,40);
for index=1:40
    toa_V=toa_dt_comp(:,index)';
    toa_COEF(:,:,index)=cwt(toa_V,1:48,'db4');
end

%% %%%%%%%%%%%%%%  standard deviation based on blades %%%%%%%%%%%%%%
```

```
toa_Sd=zeros(48,40);
for ii=1:40
    toa_Sd(:,ii)=std(toa_COEF(:,:,ii),0,2);
end

figure(3)
surf(toa_Sd);grid on;title('standard deviation of TOA coefficients');
zlabel('STD of WT Coef')
ylabel('scales')
xlabel('blade#')

%% %%%%%%%%%%%% Kurtosis of WT Coef based on the blades %%%%%%%%%%%%%%%

toa_kurtosis=zeros(48,40);
for ii=1:40
    toa_kurtosis(:,ii)=kurtosis(toa_COEF(:,:,ii),0,2);
end
figure(4);
surf(toa_kurtosis);grid on;title('Kurtosis of TOA WT coefficients');
ylabel('Scales')
xlabel('Blade#')
zlabel('Kurtosis of WT Coef')

%% %%%%%%%%%% wavelet coefficient based on the cycles %%%%%%%%%%%%%%%%%

toa_COEF=zeros(48,40,1408);
for index=1:1408
    toa_V=toa_comp(index,:);
    toa_COEF(:,:,index)=cwt(toa_V,1:48,'db4');
end

%% %%%%%%%%%%%% standard deviation based on cycles %%%%%%%%%%%%%%%%%%

toa_Sd=zeros(48,1408);
for ii=1:1408
    toa_Sd(:,ii)=std(toa_COEF(:,:,ii),0,2);
end
```

```
figure(3)
surf(toa_Sd,'EdgeColor','none');grid on;title('standard deviation of
TOA coefficients','fontsize',14,'fontweight','bold');
zlabel('STD of WT Coef','fontsize',16,'fontweight','bold')
ylabel('scales','fontsize',16,'fontweight','bold')
xlabel('cycle#','fontsize',16,'fontweight','bold')

%% %%%%%%%%%%%%%%%% Kurtosis based on cycles %%%%%%%%%%%%%%%%%%%%

toa_kurtosis=zeros(48,1408);
for ii=1:1408
    toa_kurtosis(:,ii)=kurtosis(toa_COEF(:,:,ii),0,2);
end

figure(4)
surf(toa_kurtosis,'EdgeColor','none');grid on;title('Kurtosis of TOA
coefficients','fontsize',14,'fontweight','bold');
zlabel('Kurtosis of WT Coef','fontsize',16,'fontweight','bold')
ylabel('scales','fontsize',16,'fontweight','bold')
xlabel('cycle#','fontsize',16,'fontweight','bold')
```

APPENDIX B

```
clc;close all;clear all;
tc=xlsread('tc_modified');
% x(1408x40)=preprocessed TC
% y(1408x40)=integrated time series
% y_fit=local trend in each bin with respect to x_fit which is 1:n
% x_bin=TC amount in each bin

%% %%%%%%%%%%%%%%%%%%%%% preprocessing data %%%%%%%%%%%%%%%%%%%%%%%%%

TC_avg_blade=(mean(tc,2));      % mean value of a row(cycle) of TC
TC_comp=tc-repmat(TC_avg_blade,1,40);

%% %%%%%%%%%%%% first harmonic fourier coef's %%%%%%%%%%%%%%%%%%%

a=zeros(1408,1);
b=zeros(1408,1);
for ii=1:1408
        for jj=1:40
            a(ii)=(1/10)*(a(ii)+TC_comp(ii,jj)*cos((jj-1)*pi/20));
            b(ii)=(1/10)*(b(ii)+TC_comp(ii,jj)*sin((jj-1)*pi/20));
        end
end

fourier=zeros(1408,40);
x=zeros(1408,40);
for ii=1:1408
    for jj=1:40
        fourier(ii,jj)=a(ii)*cos((jj-1)*pi/20)+b(ii)*sin((jj-1)*pi/20);
        x(ii,jj)=TC_comp(ii,jj)-fourier(ii,jj);
    end
end

%% %%%%%%%%%%%%%%%% Integrated time series %%%%%%%%%%%%%%%%%%%%%%%
blade=1;
```

```
% for blade=1:40
m(blade)=mean(x(:,blade),1);    % mean value of all cycles in a blade
y=zeros(1408,40);
for j=1:1408
    for i=1:j
        y(j,blade)=y(j)+x(i,blade);
    end
    y(j,blade)=y(j,blade)-j*m(blade);
end

%% %%%%%%%%%%%%%%%% local trend in each n-point box %%%%%%%%%%%%%%%%
y_fit=zeros(1408,40,10);
for n=3:12
    N=1408/n;
    X_FIT=(1:1:n);
    X_BIN=zeros(n,1);
   for i=1:n:(n-1)*N
     for j=i:i-1+n
             X_BIN(j-i+1)=x(j,blade);
     end

     for j=i:i+n-1
       p=polyfit(X_FIT,X_BIN',1);
       y_fit(j,blade,n-2)=p(1)*j+p(2);
     end
   end
end



 %% %%%%%%%%%%%%%%%% DEFLACTUATION FUNCTION %%%%%%%%%%%%%%%%%%%%%%%%

DF_FUNCTION=zeros(1301,40,10);       %detrend function in each box
for j=1:1301
    DF_FUNCTION(j,blade,n-2)=y(j,blade)-y_fit(j,blade,n-2);
end
 for n=3:12
    F(n)=var(DF_FUNCTION(:,blade,n-2));
```

```
    B(n)=log(n);
    C(n)=log(F(n));
    figure(blade);
    plot(B,C,'--ks');xlim([1,2.5]);
    hold on;
%     figure(blade);
%     plot(log(n),log(F(n)),'-
bs');xlabel('log(n)');ylabel('log(F(n))');  %,'markeredgecolor','k'
%     hold on;
end
```